J Geotechnical Testing, Sept. 2002, Vol. 25, No. 3
Paper ID GTJ20029678_253
Available online at: www.astm.org

Man Feng,[1] *Delwyn G. Fredlund,*[2] *and Fangsheng Shuai*[3]

A Laboratory Study of the Hysteresis of A Thermal Conductivity Soil Suction Sensor

ABSTRACT: An experimental program was set up to study the capillary hysteresis of the ceramic block for a newly developed thermal conductivity soil suction sensor. The testing program included two series of tests: one series of tests measured the capillary hysteresis of the ceramic blocks and the other measured the hysteresis of the relationships between the suction sensor output and the applied suctions. Test results show that there can be approximately 40% error from the correct suction value if the conventional calibration curve is used without considering the effects of capillary hysteresis. Based on the experimental testing program, a mathematical approach, which is able to take into account the effects of capillary hysteresis, was proposed when interpreting the measured soil suction data.

KEYWORDS: matric suction, soil suction sensor, capillary hysteresis

Introduction

Field measurements of soil suction are necessary for many engineering situations, such as prediction of total heave, slope stability analysis, monitoring of moisture flux through a soil cover or liner structure, and automatic irrigation systems in agriculture. Thermal conductivity soil suction sensors appear to be one of the most promising devices for in situ measurement of soil suction (Fredlund and Rahardjo 1988; Fredlund et al. 1992). A thermal conductivity soil suction sensor consists of a cylindrical porous block containing a temperature sensing element and a miniature heater (Phene et al. 1971).

The heater at the center of the porous block converts electrical energy to thermal energy. A portion of the thermal energy will be dissipated throughout the porous block. The undissipated thermal energy will result in a temperature rise at the center of the porous block. The temperature sensor measures the temperature rise as a function of the elapsed heating time. Since water has a much higher thermal conductivity than air, the rate of dissipation of the thermal energy within the porous block will increase with the increase of water content of the porous block. A higher water content will result in a lower temperature rise at the center of the porous block, and, consequently, a lower voltage output of the temperature sensor. Since the water content is corresponding to the matric suction in the surrounding soil, the voltage output of the temperature sensor (i.e., the output of the suction sensor) can be calibrated for measuring the matric suction.

The measurement of matric suction using a thermal conductivity sensor is an indirect method. There are three relationships that indirectly relate the output of the sensor to the matric suction of the soil:

1. The output from the soil suction sensor is a voltage that is inversely proportional to the rate of dissipation of the thermal energy within the porous block;
2. The rate of dissipation of the thermal energy is dependent upon the water content of the porous block; and
3. The water content of the porous block is a function of the matric suction applied to the porous block by the surrounding soil.

The first two relationships are reversible, whereas the relationship between the water content of the porous block and matric suction in the soil exhibits hysteresis for different directions of water movement. In other words, the measured output depends upon whether water was flowing into the porous block, or out of the porous block, as the sensor proceeded toward an equilibrium condition. The hysteresis between the water content of a porous block and matric suction is usually referred to as capillary hysteresis.

As a result of the capillary hysteresis associated with water movement into, or out of the porous block of the thermal conductivity sensor, the same voltage output from the sensor can correspond to different matric suction values, depending on the drying and wetting history of the porous block. If a single drying or wetting curve is used for the calibration curve of the thermal conductivity sensor, an error will occur in the measurement when the porous block of the sensor undergoes drying and wetting cycles in the field. The influence of capillary hysteresis on the measurement of matric suction when using thermal conductivity sensors has been noticed for many years, but little research has been done on this subject (Wong et al. 1989; Fredlund 1992; Fredlund et al. 1994). Attempts were made in the present study to understand better the characteristics of capillary hysteresis in the porous block of a thermal conductivity soil suction sensor and its effects on the measurement of matric suction.

A Description of a New Thermal Conductivity Sensor

A new thermal conductivity suction sensor was developed and produced at the University of Saskatchewan for laboratory testing and field monitoring. The new sensor consists of an IC (integrated circuit) temperature sensor and a heating resistor embedded at the center of a porous ceramic block. The ceramic block has a diameter of 28 mm, a height of 38 mm, a compressive strength of ap-

[1]Golder Associates Ltd., 209-2121, Airport Drive, Saskatoon, Saskatchewan, Canada S7L 6W5.
[2, 3] Professor and Research Associate, respectively, Department of Civil Engineering, University of Saskatchewan, Saskatoon, Saskatchewan, Canada S7N 5A9.

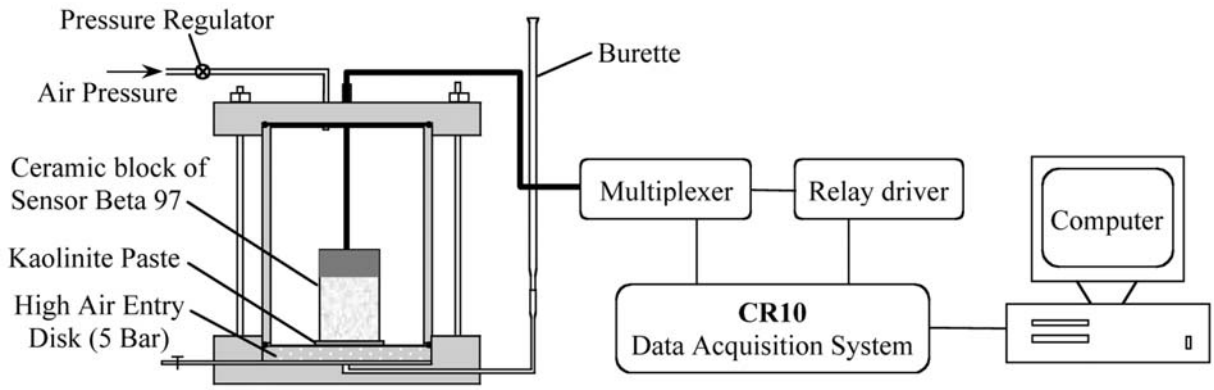

FIG. 1—*Apparatus for measuring the capillary hysteresis curves of the ceramic blocks and the relationships between suction sensor's output voltage and the corresponding matric suction.*

proximately 2100 kPa, a saturated coefficient of permeability of 2.0×10^{-6} m/s, a dry density of 0.81–0.84 Mg/m^3, and a porosity of 60–61% (Shuai et al. 1998).

Three ceramic blocks without any electronics in the ceramics (i.e., Ceramic-1 to 3), with the same dimensions as the ceramic blocks for the suction sensors, were used in the laboratory tests to investigate the capillary hysteresis of the ceramic. Six complete suction sensors (i.e., Sensor-1 to 6) were used to investigate the hysteresis associated with the relationship between the output voltage of the suction sensor and the applied matric suctions.

Test Method

Tempe type pressure plate cells were used to apply matric suction to the ceramic blocks and the suction sensors. The setup of the apparatus is shown in Fig. 1. A saturated ceramic disk with an air-entry value of 500 kPa (i.e., 5 bars) was used to separate air and water pressure. A thin layer of kaolinite paste was placed between the ceramic block and the high air-entry disk to ensure good contact and continuity of water flow between the ceramic block and the high air-entry disk.

The flow of water was monitored using a burette. At equilibrium conditions for each applied suction, the ceramic block was removed and weighed on a balance, and the water content of the ceramic block was calculated. The output voltage of the suction sensors was monitored using a CR-10 data acquisition system. Readings were taken at 1-h intervals.

Matric suctions below 10 kPa were applied by keeping the air pressure in the pressure plate cell at one atmosphere, while decreasing the water pressure below the high air-entry disk by lowering the water level in the attached burette. Matric suctions higher than 10 kPa were applied by increasing the air pressure in the pressure plate cell, while keeping the water pressure below the high air-entry disk constant.

The three ceramic blocks and the ceramic tips of the six sensors were saturated, using an applied vacuum to prevent air bubbles from being entrapped in the pores of the ceramic. The dry ceramic blocks were first placed in a vacuum chamber, and a vacuum of approximately one atmosphere was applied to the chamber for more than 2 h. Water was then sprayed into the chamber, while keeping the vacuum in the chamber constant, until the ceramic blocks were submerged in water. The vacuum was released, and the ceramic blocks were kept submerged in water for more than 4 h. The vacuum method significantly shortens the time required for saturation, while effectively preventing air bubbles from being entrapped in the ceramic.

The saturated ceramic blocks and the ceramic tips of the suction sensors were placed in the pressure plate cell. Desorption and absorption tests were conducted using the following procedure:

1. The ceramic block was dried to a maximum matric suction of 400 kPa, using applied suctions of 1, 2, 4, 7, 15, 30, 60, 100, 200, and 400 kPa, giving the initial drying curve. These applied suctions were roughly followed, and varied slightly for the actual testing conditions;
2. The applied suction was then decreased using similar stress increments in the reverse order from 400 to 0 kPa, providing data for the main wetting curve. The ceramic block was subsequently dried using the same suction increments as those in Step 1 to produce the main drying curve. The loop formed by the main wetting curve and the main drying curve is referred to as main hysteresis loop;
3. Step 2 was repeated to produce the primary drying scanning curves and the primary wetting scanning curves.

Test Results

The hysteretic behaviors of the three ceramic blocks and the six suction sensors under drying and wetting cycles in the range of 0–400 kPa are described below.

Test Results of Hysteresis Curves

Similar hysteresis curves were measured for the three ceramic blocks and for the six suction sensors. The hysteresis curves associated with Ceramic-1, Ceramic-2, Sensor-1, and Sensor-2 are shown in Figs. 2–5, respectively. When the suction was above 400 kPa, the equalization time was extremely long, extending to more than 20 days. Other factors, such as evaporation, can also start to affect the test results in this case. The drying process was stopped at an applied suction of 400 kPa.

As seen in Figs. 2–5, a relatively large gap was found to exist between the initial drying curve and the main hysteresis loop in the low suction range between 0 and 15 kPa. This indicates that a relatively large amount of air was entrapped in the pores of the ceramic when it was first wetted. The data in Tables 1 and 2 show the corresponding amounts of entrapped air.

In Table 1, w_0 and w' denote, respectively, the saturated water content of the ceramic block and the water content after rewetting

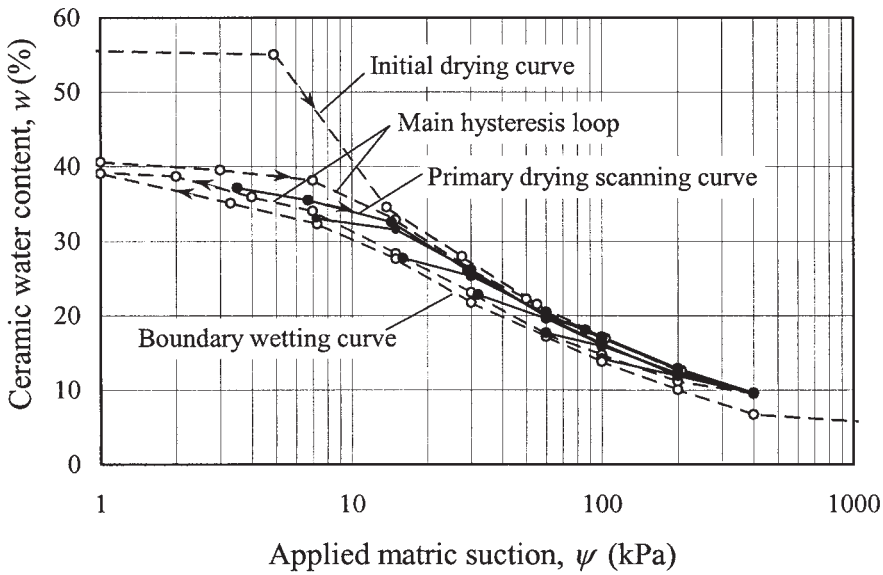

(a) Primary drying scanning curves

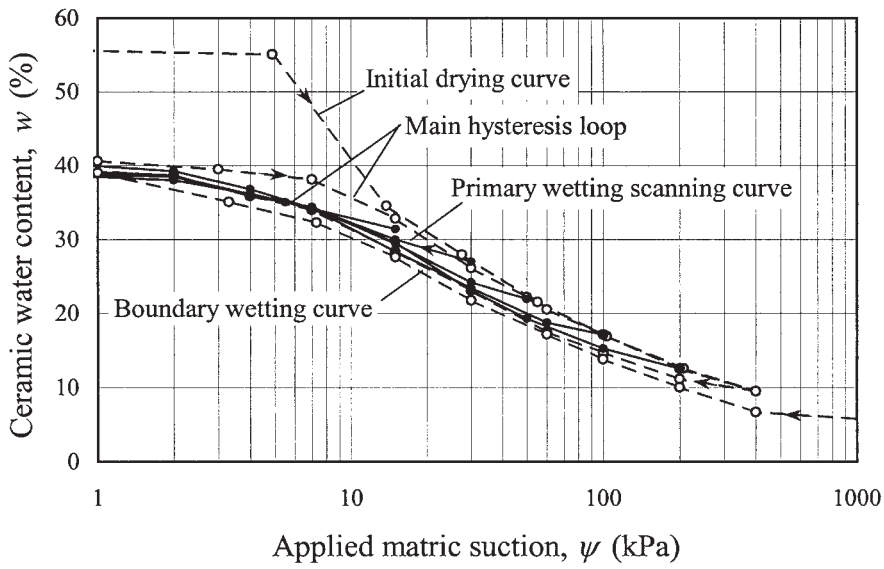

(b) Primary wetting scanning curves

FIG. 2—*The initial drying curve, main hysteresis loop, and primary scanning curves for Ceramic-1.*

to zero applied suction. The variable, S_r', represents the degree of saturation when the ceramic block is rewetted to zero applied suction. In Table 2, ΔV_0 is the sensor's output voltage change when the sensor ceramic block is fully saturated from an initially air-dried condition, and $\Delta V'$ is the sensor's output voltage change when the ceramic block is rewetted in the pressure plate cell from an air-dried condition to zero applied suction.

A degree of saturation of 70.3–73.2% was reached after the ceramic blocks were rewetted to zero applied suction. The sensor output voltage change after the sensor tip was rewetted from an air-dried condition to zero applied suction, is 76.9–90.0% of its output voltage change when the sensor tip is fully saturated from an air-dried condition. These results indicate that up to 30% of the pore space was occupied by entrapped air when the ceramic blocks were rewetted from 400 to 0 kPa.

The main hysteresis loop is always located below the initial drying curve for the water content versus applied matric suction (i.e., $w - \Psi$) relationship for the ceramic blocks. The main hysteresis loop is above the initial drying curve for the output voltage versus applied matric suction (i.e., $V - \Psi$) relationship for the suction sensors. The difference in water content (for the ceramic blocks) or output voltage (for the suction sensors) between the initial drying curve and the main drying curve varies with the applied matric suction. This difference is more significant at low matric suction range (i.e., suction lower that 15 kPa) than at higher matric suctions.

The main hysteresis loop and the primary scanning curves were found to be stable and reproducible over a two-year testing period. The thermal conductivity matric suction sensor is suitable for long-term suction measurements.

Boundary wetting curve was measured for Ceramic-1, 2, and 3, and Sensor-4, 5, and 6, by wetting an air-dried ceramic block or a suction sensor to zero applied suction. The boundary wetting curves for Ceramic-1 and 2 were shown in Figs. 2 and 3, respectively. The boundary wetting curve is close to the main wetting curve in each figure, forming the lower boundary of the hysteresis curves.

Water-Retention Characteristics of the Ceramic Block at Low Matric Suctions

The groundwater table may rise above a suction sensor installed in the field, so that the suction sensor becomes submerged. As a result, the entrapped air may escape gradually by diffusion or pore-water redistribution, and the ceramic tip will take on a water content higher than the water content corresponding to the main hysteresis loop at zero suction. Tests were conducted to study the capillary behavior of a ceramic block when it is submerged in water for a period of time.

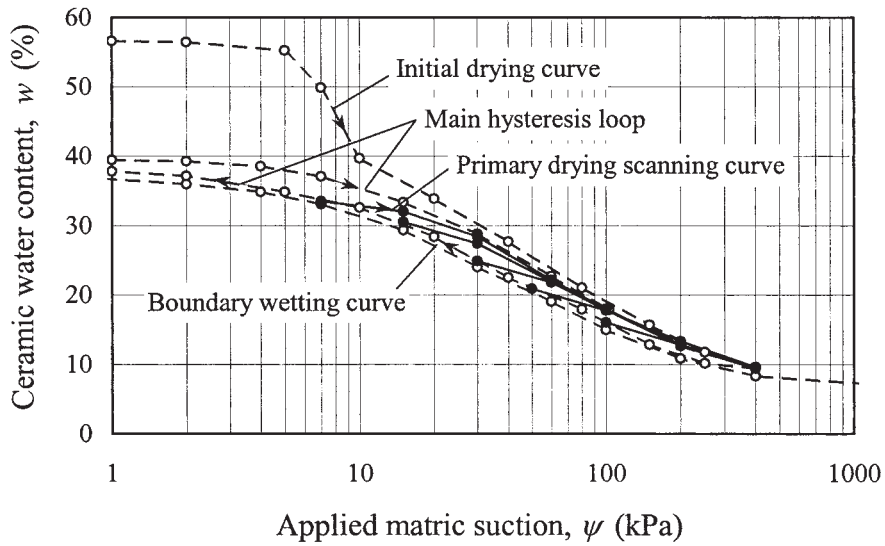

(a) Primary drying scanning curves

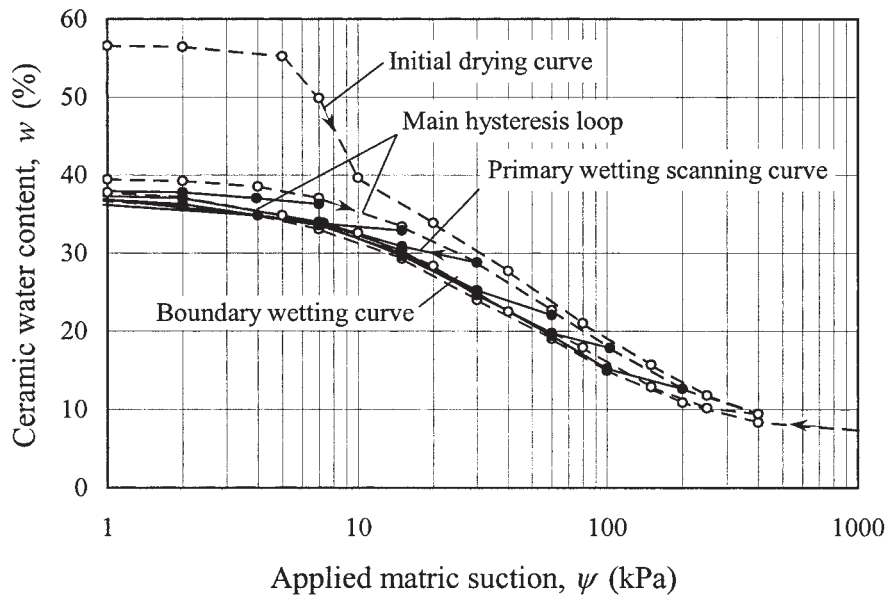

(b) Primary wetting scanning curves

FIG. 3—*The initial drying curve, main hysteresis loop, and primary scanning curves for Ceramic-2.*

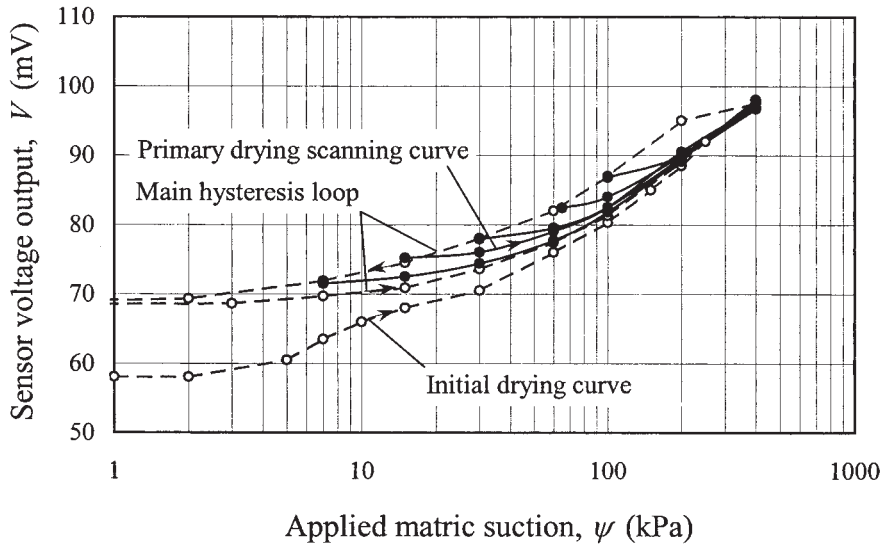

(a) Primary drying scanning curves

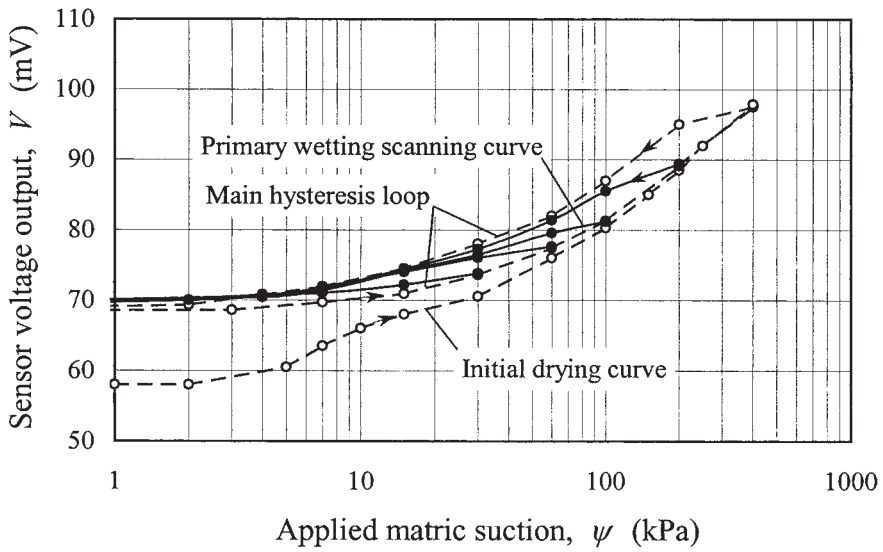

(b) Primary wetting scanning curves

FIG. 4—*The initial drying curve, main hysteresis loop, and primary scanning curves for Sensor-1.*

Long-Term Submergence of the Ceramic Blocks in Water—An air-dried ceramic block was soaked in de-aired water, while the change in water content of the ceramic block with time was measured. Two ceramic blocks were tested at various times, including Ceramic-1 and a ceramic block that had not been used in the above tests, referred to as Ceramic-4. Ceramic-1 was fully submerged while Ceramic-4 was half submerged. Figure 6 shows the increase in water content with time for the two ceramic blocks. The two curves have a similar shape. An interesting phenomenon is that the two curves have a turning point occurring at an elapsed time of 1–2 h. Before this point, the water content shows a rapid increase with time. Immediately after this point is passed, the rate of increase in water content slows down significantly, though the water content still shows a continuous increase. Equilibrium was still not reached at an elapsed time of 1800 h (2.5 months) for Ceramic-4. The degree of saturation of Ceramic-1 was 73.6% after eight days of submergence, and the degree of saturation of Ceramic-4 is 75.1% after 2.5 months of submergence.

The degree of saturation was 63.5% at the turning points on the water content versus time curves for Ceramics-1. This is even lower than the degree of saturation at the point of zero matric suction on the main hysteresis loop, which was 73.2%. After eight days of submergence, the degree of saturation of Ceramic-1 was close to that of the point of zero matric suction on the main hysteresis loop.

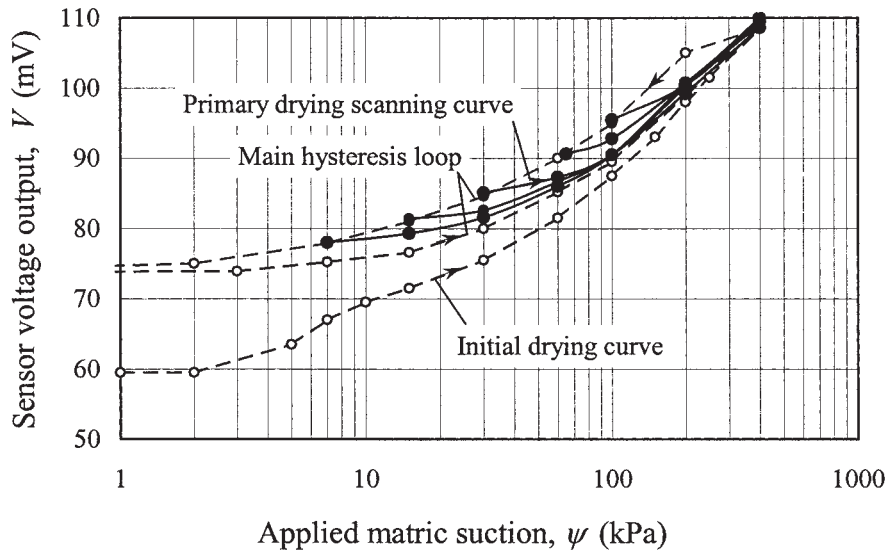

(a) Primary drying scanning curves

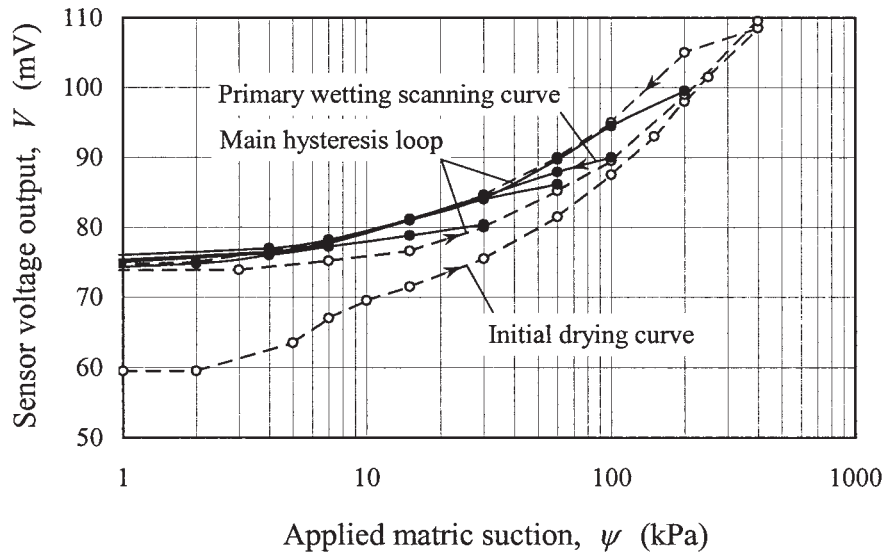

(b) Primary wetting scanning curves

FIG. 5—*The initial drying curve, main hysteresis loop, and primary scanning curves for Sensor-2.*

TABLE 1—*Water content after initial drying and rewetting to an applied suction of 0.2 kPa.*

Specimen	θ_0 (%)	θ' (%)	S_r' (%)
Ceramic-1	41.0	56.0	73.2
Ceramic-2	40.0	56.5	70.8
Ceramic-3	41.5	59.0	70.3

TABLE 2—*Voltage output after initial drying and rewetting to an applied suction of 0.2 kPa.*

Specimen	ΔV_0 (*mV*)	$\Delta V'$ (*mV*)	$\Delta V'/\Delta V_0$ (%)
Sensor-1	54.0	43.0	79.6
Sensor-2	68.0	53.0	77.9
Sensor-3	65.0	50.0	76.9
Sensor-4	65.3	58.8	90.0
Sensor-5	61.3	53.3	86.9
Sensor-6	56.1	49.1	87.5

The existence of the turning point on the above curves would appear to be related to the pore structure of the ceramic. Before the turning point is reached, the airflow paths still exist in the ceramic block. The pore-air can easily flow out of the ceramic, resulting in a rapid change in content. At the turning point, the water content reaches a value such that the airflow paths start to be restricted. With a further increase in water content, the remaining pore-air is entrapped in the pores as air bubbles. However, since there is an energy difference between the entrapped air and the air in the atmosphere outside the ceramic, the entrapped air will attempt to escape from the ceramic by diffusion and pore-water redistribution. The water content shows a continuous but slow increase with respect to time. The "escaping" of entrapped air and the increase in water content are processes lasting over an extremely long time.

Wetting and Drying of the Ceramic Block in Low Suction Range—If the ceramic block has been submerged for a prolonged period of time, the water content of the ceramic block will be higher than the water content at zero matric suction on the main hysteresis loop. The subsequent drying curve will be above the main drying curve. Tests were also carried out to simulate the drying and wetting behavior of the ceramic tip after a prolonged submergence. Figures 7 and 8 show the results of drying and wetting when the ceramic was initially saturated and initially unsaturated, respectively.

In the test results shown in Fig. 7, the ceramic block was saturated using the vacuum method, followed by two drying and wetting cycles. The applied suction was increased in three increments to 7 kPa and then decreased back to zero, forming the first cycle

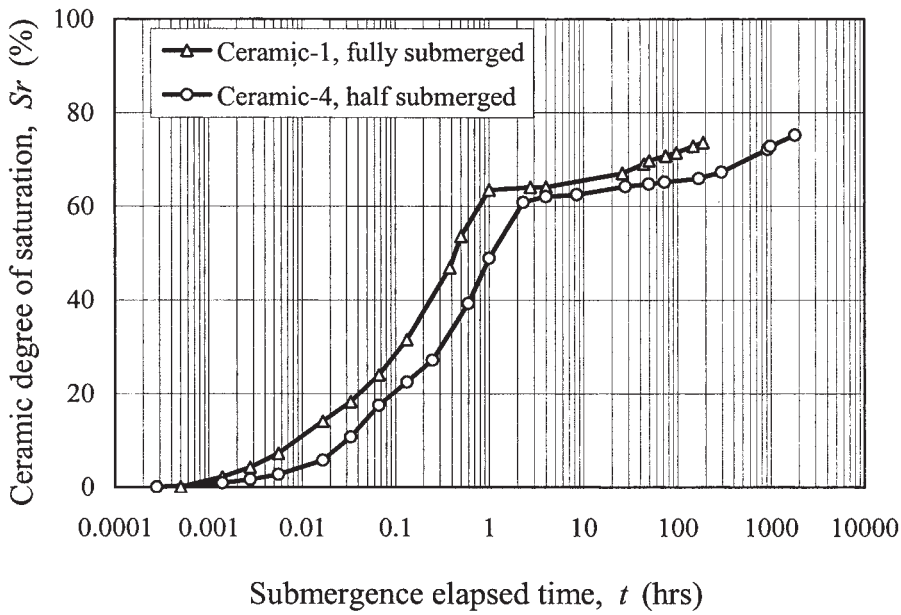

FIG. 6—*The increase in water content with time of ceramics submerged in water.*

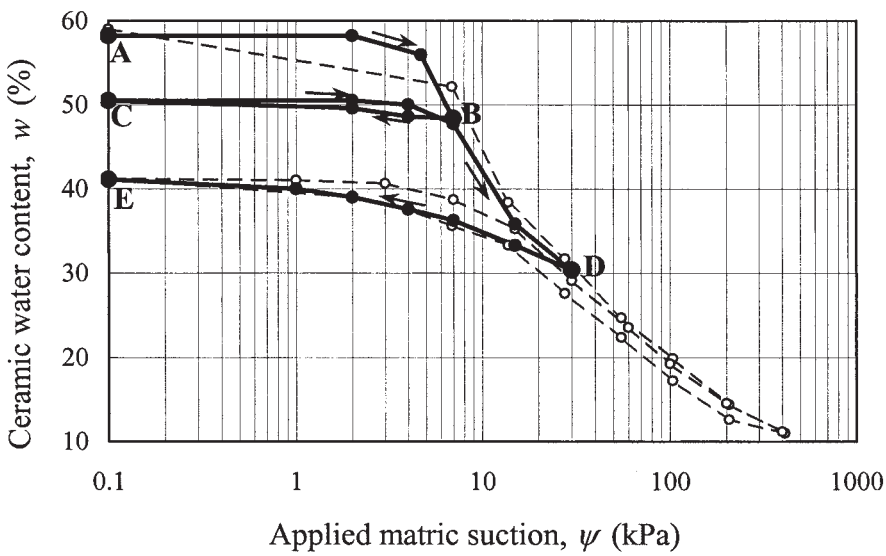

FIG. 7—*Wetting and drying outside the main hysteresis loop for Ceramic-1: Case-I.*

(i.e., Line ABC in Fig. 7). The ceramic block was then dried to a suction of 30 kPa, and subsequently rewetted to zero suction, forming the second cycle (i.e., Line CDE in Fig. 7).

In the drying process of the first cycle, the water content versus applied suction (i.e., $w - \Psi$) relationship follows the initial drying curve. The wetting curve is almost horizontal. This would tend to indicate that, if the water content of the ceramic is in the gap area between the initial drying curve and the main drying curve, wetting of the ceramic takes place mainly through the escape of entrapped air or so-called relaxation.

During the second cycle of drying and wetting, the ceramic block was redried to a point of 30 kPa, which is below the gap area. The rewetting curve essentially coincides with the main wetting loop. This indicates that a dry-installed ceramic suction sensor, unless it is flooded for a long period of time (approximately ten days for the new suction sensor), will not reach a water content in the area above the main hysteresis loop (i.e., in the gap area). The wetting and drying will take place within the hysteresis loop. Even when the prolonged submergence does occur, a small suction (e.g., 15 kPa for the new suction sensor) can bring the drying and wetting back to the main hysteresis loop. A saturated-installed suction sensor will also behave within the main hysteresis loop, after it reaches a certain value of suction (e.g., 15 kPa for the new suction sensor) in any drying process.

Figure 8 shows the drying and wetting of an initially unsaturated ceramic (Ceramic-2). The shape of the drying and wetting curves in the low suction range in Fig. 8 provides a further support of the above conclusions drawn from Fig. 7.

Discussions of the Test Results

Considerable research work has been done previously on the calibration of the thermal conductivity sensor (Fredlund and Wong 1989; Fredlund 1992). Conventionally, the ceramic tip of the suction sensor was first submerged in a water bath for a few days. The sensor was then mounted in a pressure plate cell, and matric suctions were applied by increasing the air pressure in the pressure plate cell incrementally, while maintaining a constant water pressure below the high air-entry disk. The measured calibration curve using the conventional method was a drying curve.

There are two problems associated with the conventional calibration procedure. The first problem is that the initial degree of saturation of the ceramic tip is not known. Experiments in this study showed that a degree of saturation of only 75.1% was reached for a ceramic block after 2.5 months of submergence in water, and the degree of saturation was still increasing with time (Fig. 6). Therefore, the calibration curve could be anywhere between the initial drying curve and the main drying curve, or even below the main drying curve, depending on how long the ceramic tip was submerged.

The second problem associated with the conventional calibration curve is that this curve is only a drying curve. It does not take into consideration the effects of capillary hysteresis. When a suction sensor is installed in the field, the ceramic tip of the suction sensor will experience numerous drying and wetting cycles, depending upon the moisture movement in the surrounding soil. For a certain value of voltage output from the suction sensor, the corresponding matric suction could be anywhere between the main drying curve and the main wetting curve, or even between the initial drying curve and the main wetting curve, depending on the water flow history. Therefore, if only a drying curve is used as the calibration curve, an error will occur as a result of capillary hysteresis.

Since drying and wetting take place mainly within the main hysteresis loop for most field conditions, the following discussions do not take into consideration the drying and wetting outside the main hysteresis loop. Assuming that the main drying curve is the calibration curve, the maximum possible error will occur when the ceramic tip is undergoing a main wetting process at the time the voltage reading is taken. Let us suppose that the actual suction is Ψ_w and the measured suction is Ψ_d. The maximum possible relative error will be

$$\varepsilon_{\max} = \frac{\delta\Psi_{\max}}{\Psi_w} = \frac{\Psi_d - \Psi_w}{\Psi_w} \tag{1}$$

where

Ψ_d = suction on the main drying curve corresponding to a certain output (i.e., the measured suction if the main drying curve is used as the calibration curve), and

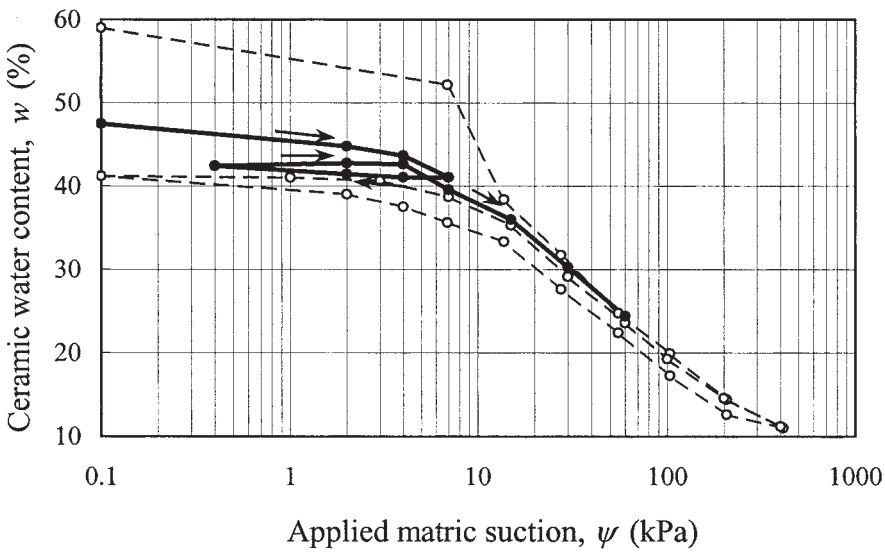

FIG. 8—*Wetting and drying outside the main hysteresis loop for Ceramic-1: Case-II.*

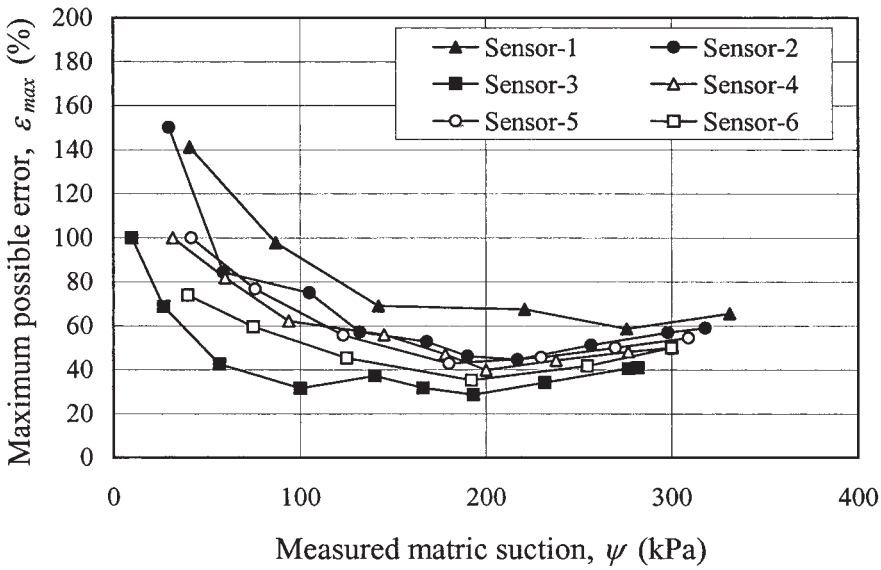

FIG. 9—*Maximum possible errors caused by the capillary hysteresis for the six suction sensors when the main drying curves are used as calibration curves.*

Ψ_w = suction on the main wetting curve corresponding to the same output, and is the actual suction if the ceramic tip of the sensor is undergoing a main wetting process.

Figure 9 shows the relationship between the maximum possible relative error, ε_{max}, and the measured matric suction, Ψ_d, for the six sensors when the main drying curve is used as the calibration curve.

It can be seen that the maximum possible error decreases with suction when the measured suctions are low. The maximum errors are approximately constant when the measured suctions exceed 100 kPa. The average maximum possible error varies from sensor to sensor, from 30% for Sensor-3 up to more than 60% for Sensor-1 when the measured suctions are higher than 100 kPa. The above discussion indicates that the effect of capillary hysteresis on the measurement of matric suction, when using thermal conductivity suction sensors, is significant.

The calibration curve measured using the conventional method of calibration could be above or even below the main drying curve, depending on the length of submergence. The error in the measurement when using a calibration curve obtained using the conventional calibration procedure could be even higher than that indicated in Fig. 9.

Prediction of Hysteresis Curves

The experimental evidence would indicate that hysteresis should be taken into consideration when calibrating the thermal conductivity soil suction sensors. It is, however, impractical to measure all the hysteresis curves along the calibration range. It is desirable to develop an appropriate mathematical approach that can estimate the hysteresis curves from a limited amount of calibration data.

Several hypothetical hysteresis models have been proposed in the research literature. An examination of some of the models using the measured hysteresis data of the new suction sensors showed that the models either require too much calibration data or cannot provide a reasonable prediction of hysteresis (Feng 1999).

The experimental results showed that the hysteresis curves were consistent for all ceramic blocks. The six suction sensors and the three ceramic blocks tested all had similar hysteresis curves. It would seem logical to predict the hysteresis curves of other sensors that have only limited calibration data by using a proper formulation that fits the measured calibration curves of the sensors with known hysteresis curves. The following equation is proposed to fit the main drying and main wetting curves (Shuai et al. 1998).

$$w(\psi) \text{ or } V(\Psi) = \frac{ab + c\Psi^d}{b + \Psi^d} \tag{2}$$

This equation fits well the measured main drying and main wetting curves within the measured suction range (i.e., 0–400 kPa). In Eq 2, parameter *a* corresponds to the saturated water content, or the sensor reading when the suction is zero on the main hysteresis loop. Parameter *c* corresponds to the residue water content or the sensor reading when the ceramic tip of the sensor is in a dry condition. Parameters *a* and *c* are easy to measure and remain the same for the main wetting and main drying curves. With one branch of the main hysteresis loop measured, two parameters, *b* and *d*, remain unknown for the other branch. If two points on the unknown branch are measured, this branch can be estimated using Eq 2.

With one branch of the main hysteresis loop measured and the other branch estimated, the following equations are used to fit the scanning curves.

$$w_d(\Psi, \Psi_1) = w_d - \left(\frac{\Psi_1}{\Psi}\right)^{\alpha} (w_d - w_w) \tag{3}$$

$$w_w(\Psi, \Psi_1) = w_w + \left(\frac{\Psi}{\Psi_1}\right)^{\alpha} (w_d - w_w) \tag{4}$$

where

$w_d(\Psi, \Psi 1)$ = water content at suction Ψ on the drying scanning curve that starts at a suction value, Ψ_1;
$w_w(\Psi, \Psi 1)$ = water content at suction Ψ on the wetting scanning curve that starts at a suction value, Ψ_1.

There is one unknown, empirical parameter α in the above equations. This parameter α determines the degree of curvature of the scanning curves.

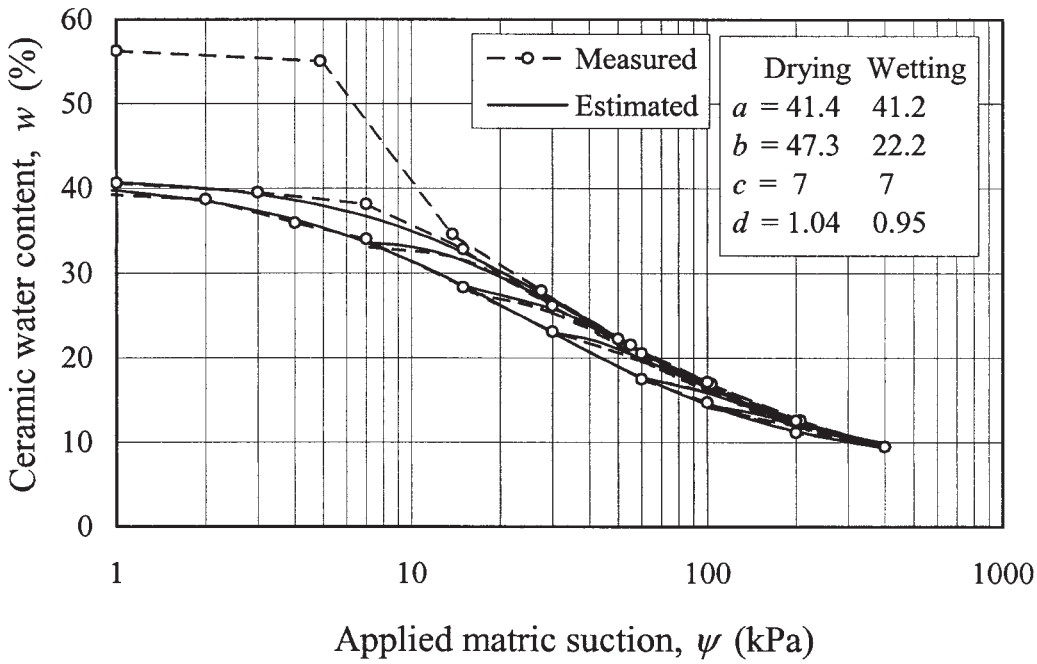

(a) Primary drying scanning curves

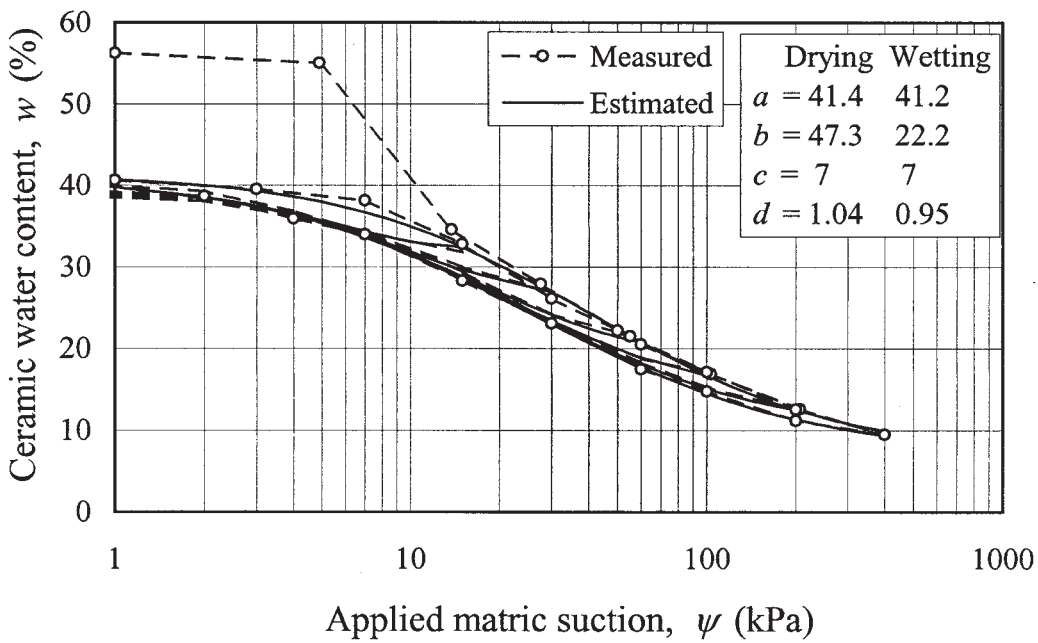

(b) Primary wetting scanning curves

FIG. 10—*Measured and estimated primary scanning curves for Ceramic-1.*

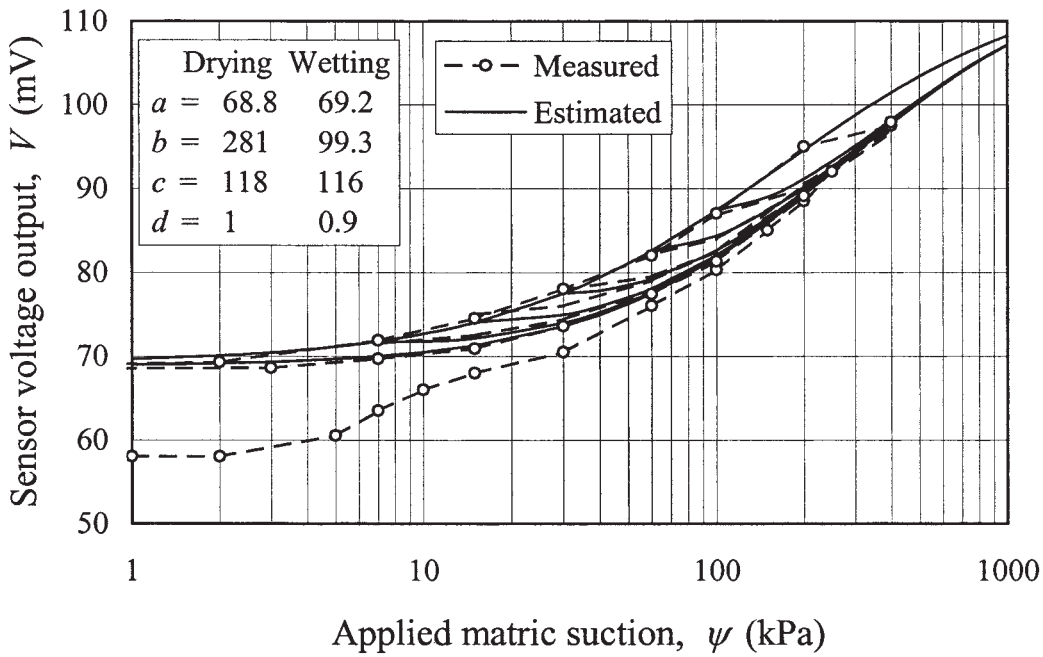

(a) Primary drying scanning curves

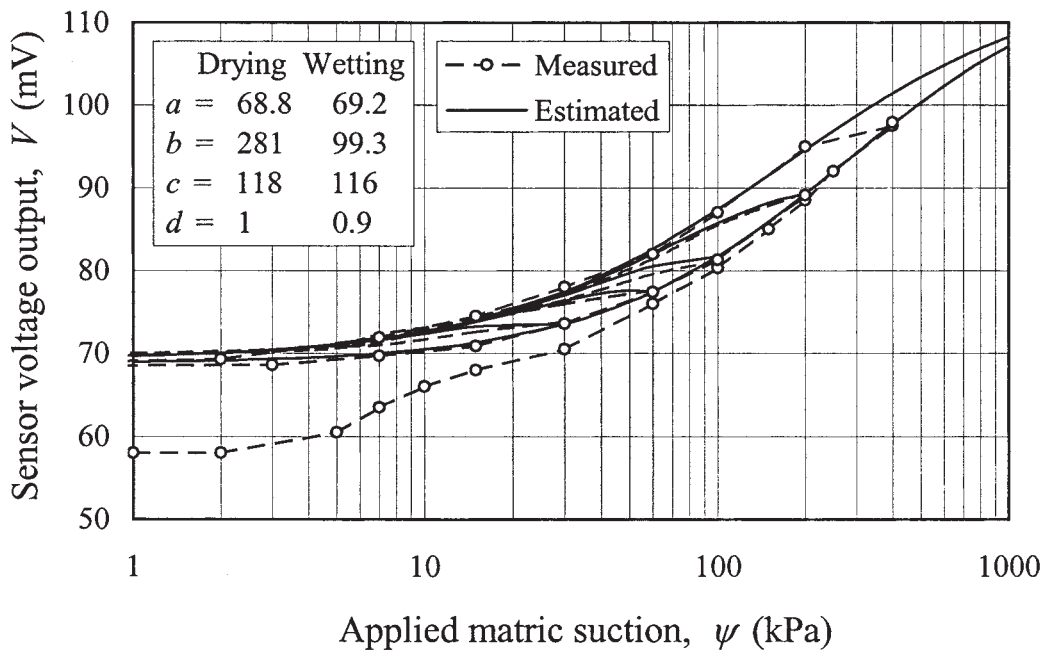

(b) Primary wetting scanning curves

FIG. 11—*Measured and estimated primary scanning curves for Sensor-1.*

The measured hysteresis curves of the three ceramic blocks and the six suction sensors were fitted using Eqs 2–4. The predicted curves of the main hysteresis loop and primary scanning curves for Ceramic-1 and Sensor-1 are shown in Figs. 10 and 11, respectively.

The best-fit value for α appears to be 1.8. A value of α equal to 1.8 was used for both the primary drying scanning curves and the primary wetting scanning curves of all the three ceramic blocks and six suction sensors. It can be seen in Figs. 10 and 11 that the predicted primary scanning curves are close to the measured scanning curves. The α value of 1.8 appears to be reasonable for predicting the primary scanning curves for other suction sensors.

It should be noted, however, that the value of 1.8 for the parameter α is valid only for the new thermal conductivity suction sensors that were used in this study. The α value could be different for other suction sensors. It is necessary to investigate the hysteresis properties using some typical sensors to estimate the α value for other types of sensors under consideration.

Conclusions

The laboratory testing program showed that the hysteresis curves of the new thermal conductivity soil suction sensors and the ceramic blocks were stable and reproducible over a two-year experimental period. The thermal conductivity sensors appear to be a reliable means for long-term measurement of laboratory and in situ matric suctions.

Calibration forms a crucial step towards the utilization of the thermal conductivity soil suction sensors. This study shows that, if the conventional calibration procedure is used to obtain the calibration curve, the error caused by the capillary hysteresis of the ceramic will be unacceptable.

The following procedure is recommended in calibrating the Beta 97 sensors:

1. Saturate the sensor ceramic tip by submerging it in water for more than one day.
2. Install the suction sensor in a pressure plate cell and apply a suction of 50–100 kPa.
3. After equilibrium, reduce the suction to zero.
4. After equilibrium, increase the suction in increments following the conventional calibration procedure to measure the main drying curve.
5. Rewet the sensor ceramic to obtain two points on the main wetting curve.

The main wetting curve is estimated using Eq 2. The primary scanning curves are estimated using Eqs 3 and 4, using an α value of 1.8.

A similar procedure can be used to calibrate other thermal conductivity soil suction sensors. However, a study of the hysteretic properties of the ceramic block should be conducted to best estimate the value of the α parameter for Eqs 3 and 4.

References

Feng, M., 1999, "The Effects of Capillary Hysteresis on the Measurement of Matric Suction Using Thermal Conductivity Sensors," Master of Science Thesis, University of Saskatchewan, Saskatoon.

Fredlund, D. G., 1992, "Background, Theory, and Research Related to the Use of Thermal Conductivity Sensors for Matric Suction Measurement," in *Advance in Measurement of Soil Physical Properties*: *Bringing Theory into Practice*, SSSA Special Publication No. 30, pp. 249–261.

Fredlund, D. G., Gan, J. K.-M., and Li, W.-X., 1994, "Thermal Conductivity Suction Sensor - Design Considerations," in *Proceedings, 13th International Conference, Soil Mechanics Foundation Engineering*, New Delhi, India, pp. 291–296.

Fredlund, D. G. and Rahardjo, H., 1988, "State-of-Development in the Measurement of Soil Suction," in *Proceedings, First International Conference, Engineering Problems of Regional Soils*, Beijing, China, pp. 582–588.

Fredlund, D. G., Sattler, P. J., and Gan, J., 1992, "In Situ Suction Measurement Using Thermal Conductivity Sensors," in *Proceedings, 7th International Conference, Expansive Soils*, Dallas, TX, pp. 325–330.

Fredlund, D. G. and Wong, D. K. H., 1989, "Calibration of Thermal Conductivity Sensors for Measuring Soil Suction," *Geotechnical Testing Journal*, Vol. 12, No. 3, pp. 188–194.

Phene, C. J., Hoffman, G. J., and Rawlins, S. L., 1971, "Measuring Soil Matric Potential *In Situ* by Sensing Heat Dissipation within a Porous Body: i. Theory and Sensor Construction," *Soil Science Society of America, Proceedings*, Vol. 35, pp. 27–33.

Shuai, F., Yazdani, J., Feng, M., and Fredlund, D. G., 1998, *Supplemental Report on the Thermal Conductivity Matric Suction Sensor Development (Year II)*, Department of Civil Engineering, University of Saskatchewan, Saskatoon, Canada.

Wong, D. K. H., Fredlund, D. G., Imre, E., and Putz, G., 1989, "Evaluation of AGWA-II Thermal Conductivity Sensors for Soil Suction Measurements, Transportation Research Record 1219," Transportation Research Board, National Research Council, Washington, DC, pp. 131–143.